

Identifiability and Reconstruction of Shapes from Integral Invariants

T. Fidler¹, M. Grasmair¹, O. Scherzer^{1,2}

¹ Institute of Computer Science, University of Innsbruck, Technikerstraße 21a,
A-6020 Innsbruck, Austria.

² Johann Radon Institute for Computational and Applied Mathematics,
Altenberger Str. 69, A-4040 Linz, Austria.

Thomas.Fidler@uibk.ac.at.
Markus.Grasmaier@uibk.ac.at.
Otm.Scherzer@uibk.ac.at.
October 12, 2007

Abstract

Integral invariants have been proven to be useful for shape matching and recognition. As we have pointed out in a recent paper, fundamental mathematical questions have not been addressed in the computer vision literature. In this article we are concerned with the identifiability and numerical algorithms for the reconstruction of a star-shaped object from its integral invariant. In particular we analyze two integral invariants and prove injectivity for one of them. Additionally, numerical experiments are performed.

Keywords: integral invariants

1 Introduction

Integral invariants and corresponding signatures have been introduced by Manay et al. [4], see also [7] for applications, as a tool for shape matching and classification. The results presented in the cited articles indicate their usefulness as alternative to differential invariants in the above mentioned applications, when data errors may be present.

Contrary to the field of differential invariants, where vast amounts of literature exist (see the reference list in [4]), hardly any analytical results on the integral counterparts have been published. In particular, the question whether a shape can be uniquely determined by a suitable integral invariant (see [1]) has not been treated yet.

In the following we discuss this question for two integral invariants presented in [1], the *cone* and the *circular* area invariant. In particular, we consider the case, where the object Ω , the invariant of which is to be computed, is star-shaped with respect to a specified reference point \mathbf{x}_0 , that is,

$$\Omega = \{ \mathbf{x}_0 + t\varphi : 0 \leq t < \gamma(\varphi), \varphi \in \mathbb{S}^{n-1} \} \subset \mathbb{R}^n$$

for some given radial function $\gamma : \mathbb{S}^{n-1} \rightarrow \mathbb{R}_{>0}$. Thus, the set Ω can be identified with the function γ . Moreover, it is natural to regard the invariant of Ω as a mapping on the sphere as well.

It is shown in Lemma 3 that, up to a nonlinear (but rather trivial) transformation, the cone area integral invariant for star-shaped objects is equivalent to computing integrals of the radial function over spherical caps. The question, whether a function on \mathbb{S}^{n-1} is uniquely determined by its integrals over all spherical caps of a given aperture ε has been treated in [5], where the uniqueness is proven for all but countably many apertures $0 < \varepsilon < 2\pi$ (cf. Theorem 5).

Although this result shows that the required injectivity holds in the case of the cone area integral invariant, new problems arise by closer investigation of the properties of the invariant. First, although the set of parameters where the injectivity does not hold is small, it is nevertheless dense in the interval $(0, 2\pi)$ of all possible apertures. Thus, every implementation of the cone area invariant could lose the injectivity property because of unavoidable numerical inaccuracies. Second, it can be shown that the invariant is compact when regarded as operator $J : L^n(\mathbb{S}^{n-1}) \rightarrow L^1(\mathbb{S}^{n-1})$, which implies that its inverse can never be continuous.

For further investigations on the invertibility of J , we consider the inverse problem of solving the operator equation $J[\gamma] = J^0$, where $J^0 \in L^n(\mathbb{S}^{n-1})$ is some given data. In other words, we try to (numerically) reconstruct an object from a given invariant. For the reconstruction we employ an iterative regularization technique.

The second part of the article is concerned with the circular area integral invariant, which is defined as the area of intersection of Ω with balls of a given radius $R > 0$ centered at the boundary of the object. Here the situation is different, since, contrary to the cone invariant, no injectivity results are available. The reason for this is the rather complex structure of the invariant when formulated as function on the sphere. Thus, we directly employ nonlinear Landweber iteration for the solution of the operator equation $J[\gamma] = J^0$.

To substantiate the applicability of the presented theoretical results, we present for each discussed integral invariant the output of the numerical experiments at the end of the corresponding section.

2 Integral Invariants

In this section we recall the definitions of integral invariants given in [1].

Definition 1. *Let $f : \mathbb{R}_{\geq 0} \times \mathbb{R}^n \rightarrow \mathbb{R}$ satisfy the following conditions:*

- *For every $r \geq 0$ the function $\mathbf{x} \mapsto f(r, \mathbf{x})$ is locally summable.*
- *For every compact subset $K \subset \mathbb{R}^n$ and $r_0 \geq 0$ we have*

$$\lim_{r \rightarrow r_0} \int_K |f(r, \mathbf{x}) - f(r_0, \mathbf{x})| d\mathcal{L}^n(\mathbf{x}) = 0.$$

- *The function f is rotationally symmetric around \mathbf{e}_1 , that is, $f(r, \mathbf{x}) = f(r, U\mathbf{x})$ whenever $U \in O(n)$ is an orthogonal matrix satisfying $U\mathbf{e}_1 = \mathbf{e}_1$.*

In the following we refer to a function f satisfying above conditions as kernel function.

Definition 2. Let f be a kernel function. For an open and bounded subset $\Omega \subset \mathbb{R}^n$ with Lipschitz boundary $\partial\Omega$ and $\mathbf{x}_0 \in \mathbb{R}^n$ we define a mapping $I[\Omega] : \partial\Omega \rightarrow \mathbb{R}$ by

$$I[\Omega](\mathbf{x}) := \int_{R_{\mathbf{x}-\mathbf{x}_0}(\Omega-\mathbf{x}_0)} f(\|\mathbf{x}-\mathbf{x}_0\|, \mathbf{y}) d\mathcal{L}^n(\mathbf{y}),$$

where $R_{\mathbf{y}} : \mathbb{R}^n \rightarrow \mathbb{R}^n$ is any rotation satisfying $R_{\mathbf{y}}\mathbf{y} = \|\mathbf{y}\|\mathbf{e}_1$.

In the definition above the point \mathbf{x}_0 may either be fixed or depend on Ω , as e.g. the choice $\mathbf{x}_0 = \text{cm}(\Omega)$ the center of mass of Ω .

A set Ω is star-shaped with respect to \mathbf{x}_0 , if there exists a function $\gamma : \mathbb{S}^{n-1} \rightarrow \mathbb{R}_{>0}$ such that

$$\partial\Omega = \{ \mathbf{x}_0 + \gamma(\boldsymbol{\varphi})\boldsymbol{\varphi} : \boldsymbol{\varphi} \in \mathbb{S}^{n-1} \}. \quad (1)$$

If Ω is a star-shaped set, then it is reasonable to regard an integral invariant not as function on $\partial\Omega$ but rather on \mathbb{S}^{n-1} . Hence, in this case we define

$$J[\gamma](\boldsymbol{\varphi}) := I[\Omega](\mathbf{x}_0 + \gamma(\boldsymbol{\varphi})\boldsymbol{\varphi}).$$

In this paper we focus on two different integral invariants, the cone area invariant and the circular area invariant. The first is defined by its kernel function

$$f_{\text{Cone}}^\varepsilon(r, \mathbf{x}) := \begin{cases} 1 & \text{if } \frac{\langle \mathbf{e}_1, \mathbf{x} \rangle}{\|\mathbf{x}\|} \leq \cos(\varepsilon/2), \\ 0 & \text{else,} \end{cases}$$

which is the characteristic function of a cone of aperture ε in direction \mathbf{e}_1 , and the latter by the kernel function

$$f_{\text{Circle}}^R(r, \mathbf{x}) := \begin{cases} 1 & \text{if } \|\mathbf{x} - r\mathbf{e}_1\| \leq R, \\ 0 & \text{else,} \end{cases}$$

which is the characteristic function of a ball of radius R around $r\mathbf{e}_1$. Here, $0 < \varepsilon < 2\pi$ and $0 < R < \infty$.

3 Cone Area Invariant

Injectivity

In the following we assume that $\Omega \subset \mathbb{R}^n$ is star-shaped with respect to \mathbf{x}_0 . For simplicity we additionally assume that $\mathbf{x}_0 = \mathbf{0}$. By $\gamma : \mathbb{S}^{n-1} \rightarrow \mathbb{R}_{>0}$ we denote the parameterization of $\partial\Omega$ defined in (1).

Lemma 3. The cone area invariant can be written as

$$J[\gamma](\boldsymbol{\varphi}) = \frac{1}{n} \int_{\text{SC}_\varepsilon^{n-1}(\boldsymbol{\varphi})} \gamma^n(\boldsymbol{\tau}) d\mathcal{H}^{n-1}(\boldsymbol{\tau}),$$

where

$$\text{SC}_\varepsilon^{n-1}(\varphi) := \{\boldsymbol{\tau} \in \mathbb{S}^{n-1} : \langle \boldsymbol{\tau}, \varphi \rangle \leq \cos(\varepsilon/2)\}$$

denotes the spherical cap in direction φ with aperture ε .

Proof. Denote by $K_\varepsilon(\varphi) = \mathbb{R}_{>0} \text{SC}_\varepsilon^{n-1}(\varphi)$ the cone with aperture ε in direction φ . Using the definition of $J[\gamma]$ we obtain by changing into polar coordinates that

$$\begin{aligned} J[\gamma](\varphi) &= \mathcal{L}^n(\Omega \cap K_\varepsilon(\varphi)) = \int_{\Omega \cap K_\varepsilon(\varphi)} d\mathcal{L}^n = \\ &= \int_{\text{SC}_\varepsilon^{n-1}(\varphi)} \int_0^{\gamma(\boldsymbol{\tau})} s^{n-1} d\mathcal{L}^1(s) d\mathcal{H}^{n-1}(\boldsymbol{\tau}) = \frac{1}{n} \int_{\text{SC}_\varepsilon^{n-1}(\varphi)} \gamma^n(\boldsymbol{\tau}) d\mathcal{H}^{n-1}(\boldsymbol{\tau}). \end{aligned}$$

□

The description of the cone area invariant derived in the lemma above proves useful both for theoretical as well as numerical reasons.

We first consider the question of injectivity of the invariant regarded as mapping $J : L_+^n(\mathbb{S}^{n-1}) \rightarrow L^1(\mathbb{S}^{n-1})$, where $L_+^n(\mathbb{S}^{n-1})$ denotes the space of all real valued functions $\gamma \in L^n(\mathbb{S}^{n-1})$ satisfying $\gamma(\varphi) \geq 0$ for almost every φ . To that end we require the notion of Gegenbauer polynomials:

Definition 4. Let $t \in (-1, 1)$, $m \in \mathbb{Z}_+$ and $\nu > 0$. The polynomials defined by

$$P_m^{[\nu]}(t) := c_m^{[\nu]} (1-t^2)^{-(\nu-1/2)} \frac{d^m}{dt^m} (1-t^2)^{m+\nu-1/2},$$

where

$$c_m^{[\nu]} := \frac{(-2)^m \Gamma(\nu+m) \Gamma(m+2\nu)}{m! \Gamma(\nu) \Gamma(2m+2\nu)}$$

are called Gegenbauer polynomials (see [6, p. 19]).

We denote by N_n the set of all zeros of all Gegenbauer polynomials $P_{m-1}^{[n/2]}$, $m \in \mathbb{N}$.

Theorem 5. Let $n \geq 3$ and $|\cos(\varepsilon/2)| < 1$. If $\cos(\varepsilon/2) \in N_n$, then there exists a function $0 \neq f \in L^1(\mathbb{S}^{n-1})$ such that

$$\int_{\text{SC}_\varepsilon^{n-1}(\varphi)} f(\boldsymbol{\tau}) d\mathcal{H}^{n-1}(\boldsymbol{\tau}) = 0 \quad \text{for all } \varphi \in \mathbb{S}^{n-1}. \quad (2)$$

Conversely, if $\cos(\varepsilon/2) \notin N_n$ and (2) holds, then $f = 0$.

Proof. See [5, p. 59].

□

In other words, Theorem 5 states that the linear functional $L_\varepsilon : L^1(\mathbb{S}^{n-1}) \rightarrow L^1(\mathbb{S}^{n-1})$,

$$L_\varepsilon[f](\varphi) := \int_{\text{SC}_\varepsilon^{n-1}(\varphi)} f(\boldsymbol{\tau}) d\mathcal{H}^{n-1}(\boldsymbol{\tau}), \quad (3)$$

is injective if and only if $\cos(\varepsilon/2) \notin N_n$.

Corollary 6. *Assume that $n \geq 3$ and $|\cos(\varepsilon/2)| < 1$. The cone area invariant $J : L_+^n(\mathbb{S}^{n-1}) \rightarrow L^1(\mathbb{S}^{n-1})$ is injective, if and only if $\cos(\varepsilon/2) \notin N_n$.*

Proof. From Lemma 3 it follows that J is the composition of the mappings $\mu_n : L_+^n(\mathbb{S}^{n-1}) \rightarrow L_+^1(\mathbb{S}^{n-1})$, $\gamma \mapsto \frac{1}{n}\gamma^n$, and L_ε . From Theorem 5 it follows that L_ε is injective if and only if $\cos(\varepsilon/2) \notin N_n$. Moreover, the mapping μ_n is bijective. This proves the claim. \square

In the case $n = 2$ an analogous result can be shown:

Theorem 7. *The mapping $J : L_+^2(\mathbb{S}^1) \rightarrow L^1(\mathbb{S}^1)$ is injective if and only if ε/π is irrational.*

Proof. In the following we regard a function $\gamma \in L^p(\mathbb{S}^1)$ as 2π -periodic function $\tilde{\gamma} \in L_{\text{loc}}^1(\mathbb{R})$ satisfying $\int_0^{2\pi} |\tilde{\gamma}(t)|^p d\mathcal{L}^1(t) < \infty$ via the identification $\tilde{\gamma}(t) = \gamma((\cos(t), \sin(t)))$.

Assume first that ε/π is rational, e.g. $\varepsilon/\pi = k_1/k_2$ with $k_1, k_2 \in \mathbb{N}$. For $-1 < c < 1$ define $\tilde{\gamma}_c(t) := \sqrt{1 + c \cos(2k_2 t)}$. A simple calculation shows that $J[\tilde{\gamma}_c](t) = \varepsilon/2$ regardless of the value of c .

Now let ε/π be irrational. Then there exist increasing sequences $\{k_j\}_{j \in \mathbb{N}} \subset \mathbb{N}$ and $\{l_j\}_{j \in \mathbb{N}} \subset \mathbb{N}$ such that $2\pi l_j < (k_j + 1)\varepsilon < 2\pi l_j + 1/j$. Denote by $\delta_j := (k_j + 1)\varepsilon - 2\pi l_j$. Then the sequence $\{\delta_j\}_{j \in \mathbb{N}}$ converges to zero.

Thus,

$$\begin{aligned} \lim_{j \rightarrow \infty} \frac{1}{l_j} \sum_{m=1}^{k_j} J[\tilde{\gamma}](k_m \varepsilon + \varepsilon/2) &= \lim_{j \rightarrow \infty} \frac{1}{2l_j} \int_0^{(k_j+1)\varepsilon} \tilde{\gamma}^2(t) d\mathcal{L}^1(t) \\ &= \frac{1}{2} \int_0^{2\pi} \tilde{\gamma}^2(t) d\mathcal{L}^1(t) + \lim_{j \rightarrow \infty} \frac{1}{2l_j} \int_0^{\delta_j} \tilde{\gamma}^2(t) d\mathcal{L}^1(t) = \frac{1}{2} \int_0^{2\pi} \tilde{\gamma}^2(t) d\mathcal{L}^1(t) \end{aligned}$$

for every 2π -periodic function $\tilde{\gamma} \in L_{\text{loc}}^2(\mathbb{R})$. In particular, the integral of $\tilde{\gamma}^2$ over the interval $(0, 2\pi)$ is uniquely determined by the integral invariant $J[\tilde{\gamma}]$. This, however, implies that for every Lebesgue point t of $\tilde{\gamma}^2$ the value

$$\begin{aligned} \tilde{\gamma}^2(t) &= \lim_{j \rightarrow \infty} \frac{1}{\delta_j} \int_t^{t+\delta_j} \tilde{\gamma}^2(s) d\mathcal{L}^1(s) \\ &= \lim_{j \rightarrow \infty} \frac{2}{\delta_j} \left(\sum_{m=1}^{k_j} J[\tilde{\gamma}](t + k_m \varepsilon + \varepsilon/2) - l_j \int_0^{2\pi} \tilde{\gamma}^2(s) d\mathcal{L}^1(s) \right) \end{aligned}$$

is uniquely determined by $J[\tilde{\gamma}]$ as well, which implies the injectivity of J on $L_+^2(\mathbb{S}^1)$. \square

There are two noteworthy remarks to be made on the previous results: First, they all provide a necessary and sufficient condition for the injectivity of the cone area invariant. Whenever this condition fails one can construct examples of functions γ_1, γ_2 , which cannot be distinguished by means of the particular cone area invariant. Second, the set N_n is dense in $(-1, 1)$ with dense complement, which implies that arbitrarily close to every ε there are parameters where the

cone area invariant is injective as well as parameters where it is not. Thus, it can be suspected that in all cases the inverse problem of solving the operator equation $J[\gamma] = J^0$ with respect to γ for some given cone area invariant J^0 is ill-posed. In fact, it can be shown that the operator J is compact.

Inversion

In the following we treat the inverse problem of solving the equation

$$J[\gamma] = J^0$$

for some given $J^0 \in L^n(\mathbb{S}^{n-1})$. Since the operator J is compact and consequently the problem ill-posed, we apply a regularization method for its solution. For reasons of simplicity we use the nonlinear Landweber scheme (see [2]) defined by

$$\gamma_{i+1} = \gamma_i + \mu DJ[\gamma_i]^*(J^0 - J[\gamma_i]), \quad i \in \mathbb{N}, \quad (4)$$

where $\mu > 0$ denotes an appropriate constant and γ_0 an initial guess, for instance the constant function $\gamma \mapsto 1$ in case of a star-shaped domain.

In order to perform the iteration (4) we need the adjoint of the derivative of J .

Lemma 8. *The adjoint $DJ[\gamma]^* : L^{n^*}(\mathbb{S}^{n-1}) \rightarrow L^{n^*}(\mathbb{S}^{n-1})$, $n^* := n/(n-1)$, of J at $\gamma \in L_+^n(\mathbb{S}^{n-1})$ is the linear operator defined by*

$$DJ[\gamma]^*(g) = \left[\tau \mapsto \gamma^{n-1}(\tau) \int_{\text{SC}_\varepsilon^{n-1}(\tau)} g(\varphi) d\mathcal{H}^{n-1}(\varphi) \right].$$

Proof. From Lemma 3 it follows that

$$DJ[\gamma](h) = \left[\varphi \mapsto \int_{\text{SC}_\varepsilon^{n-1}(\varphi)} \gamma^{n-1}(\tau) h(\tau) d\mathcal{H}^{n-1}(\tau) \right].$$

The assertion is then a consequence of Fubini's Theorem. \square

We have also implemented an iterative Gauss-Newton scheme, but the results and the computational effort were comparable to those obtained by using the Landweber iteration.

Numerical Examples

In the following we focus on the two-dimensional case, where the boundary of the object of interest can be identified with a curve. In particular, we study two different curves which emphasize the capability of the cone area integral invariant: the first curve represents an asymmetric one with lots of details in contrast to the second one which is to a high degree symmetrical. Figure 1 shows the result of the reconstruction for both curves in the absence of noise and sufficiently many iteration steps. As can be seen on the image on the right, the reconstruction works such good that the two plots (original and reconstruction) can hardly be distinguished. The invariant of the reconstructed radial functions is shown on the left hand side of Figure 1. Additionally, we have plotted the difference between the invariants of the reconstruction and the original curve.

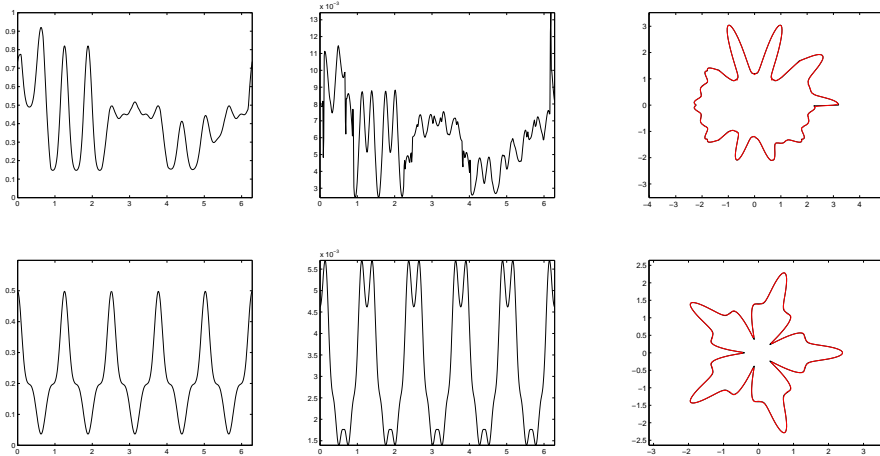


Figure 1: **(Cone area integral invariant)** *Left*: Invariant of the reconstruction. *Middle*: Residual of the invariant of the reconstruction with respect to the invariant of the original (Range: 1% of the invariant data). *Right*: Reconstructed and original curve. Parameter setting: $\mu = 0.2$, $\varepsilon = 0.2$, $n_{\text{sampling points}} = 500$ and $n_{\text{iteration steps}} = 50000$.

Since the inverse problem is known to be ill-posed the impact of noise on the reconstruction process is of interest. Table 1 lists the relative L^2 - and L^∞ -errors of the reconstructed radial functions for both curves shown in Figure 1. Also, the errors are listed in case noise is added to the integral invariant. In order to obtain satisfactory results in the presence of noise, a stopping rule for the iteration has to be implemented. To this end we compute in each step the residual $r_i := J^0 - J[\gamma_i]$. The iteration is stopped when the ratio $\|r_{i+1}\|_{L^2} / \|r_i\|_{L^2}$ exceeds for the first time the value 0.999.

Table 1: Error measures for two different curves and several noise levels. For both curves of Figure 1 the relative L^2 - and L^∞ -error of the reconstructed radial function to the original one are listed. Parameter setting: $\mu = 0.2$ and $n_{\text{sampling points}} = 500$.

Curve	Noise Level	ε	Iterations	L^2 -Error	L^∞ -Error
a	0.0%	0.2	50000	1.34%	8.94%
	2.5%	0.2	(347 ± 31)	(3.30 ± 0.08)%	(13.57 ± 0.87)%
	5.0%	0.2	(250 ± 19)	(3.89 ± 0.15)%	(14.69 ± 1.60)%
b	0.0%	0.2	50000	1.02%	2.29%
	2.5%	0.2	(898 ± 16)	(3.88 ± 0.16)%	(8.40 ± 0.31)%
	5.0%	0.2	(599 ± 21)	(5.03 ± 0.23)%	(10.74 ± 1.00)%

4 Circular Area Invariant

Inversion

In the case of the circular area invariant no injectivity results are known. Thus, we directly treat the inverse problem of solving the equation

$$J[\gamma] = J^0$$

for some given data $J^0 \in L^n(\mathbb{S}^{n-1})$, again for the case of a star-shaped set Ω . To that end we have to derive an explicit formula for the circular area invariant. Recall that the circular area invariant is the function $\varphi \mapsto \mathcal{L}^n(\Omega \cap B_R(\gamma(\varphi)\varphi))$.

Lemma 9. *Define*

$$T_\gamma(\varphi) := \{\tau \in \mathbb{S}^{n-1} : \mathbb{R}\tau \cap B_R(\gamma(\varphi)\varphi) \cap \Omega \neq \emptyset\}.$$

Then $\tau \in T_\gamma(\varphi)$ if and only if $R^2 \geq \gamma(\varphi)^2(1 - \langle \varphi, \tau \rangle^2)$ and

$$\gamma(\tau) \geq \gamma(\varphi) \langle \varphi, \tau \rangle - \sqrt{R^2 - \gamma(\varphi)^2(1 - \langle \varphi, \tau \rangle^2)}. \quad (5)$$

Proof. It is easy to show that $\mathbb{R}\tau \cap B_R(\gamma(\varphi)\varphi)$ is non-empty, if and only if $R^2 \geq \gamma(\varphi)^2(1 - \langle \varphi, \tau \rangle^2)$. In this case the intersection of $\partial B_R(\gamma(\varphi)\varphi)$ and $\mathbb{R}\tau$ consists of the points $(\gamma(\varphi) \langle \varphi, \tau \rangle \pm \sqrt{R^2 - \gamma(\varphi)^2(1 - \langle \varphi, \tau \rangle^2)})\tau$. Thus, the intersection of $\partial B_R(\gamma(\varphi)\varphi)$ with $\mathbb{R}\tau$ and Ω is non-empty if and only if (5) holds. \square

In the following we define for $\tau \in T_\gamma(\varphi)$

$$\eta(\varphi, \tau) := \sqrt{R^2 - \gamma(\varphi)^2(1 - \langle \varphi, \tau \rangle^2)}$$

and for $\varphi, \tau \in \mathbb{S}^{n-1}$

$$s(\varphi, \tau) := \begin{cases} \min\{\gamma(\tau), \gamma(\varphi) \langle \varphi, \tau \rangle + \eta(\varphi, \tau)\}, & \text{if } \tau \in T_\gamma(\varphi), \\ 0, & \text{if } \tau \notin T_\gamma(\varphi). \end{cases}$$

Lemma 10. *The circular area invariant can be written as*

$$J[\gamma](\varphi) = \frac{1}{n} \int_{\mathbb{S}^{n-1}} \operatorname{sgn}(s(\varphi, \tau)) |s(\varphi, \tau)|^n d\mathcal{H}^{n-1}(\tau).$$

Proof. Assume first that $\gamma(\varphi) < R$, which implies that $\mathbf{0} \in B_R(\gamma(\varphi)\varphi)$. Then we obtain, similarly as for the cone area invariant, that

$$\begin{aligned} J[\gamma](\varphi) &= \frac{1}{n} \int_{\mathbb{S}^{n-1}} \sup\{t > 0 : t\tau \in \Omega \cap B_R(\gamma(\varphi)\varphi)\}^n d\mathcal{H}^{n-1}(\tau) \\ &= \frac{1}{n} \int_{\mathbb{S}^{n-1}} \sup\{t : t < \gamma(\tau) \text{ and } t < \gamma(\varphi) \langle \varphi, \tau \rangle + \eta(\varphi, \tau)\}^n d\mathcal{H}^{n-1}(\tau) \\ &= \frac{1}{n} \int_{\mathbb{S}^{n-1}} s(\varphi, \tau)^n d\mathcal{H}^{n-1}(\tau). \end{aligned}$$

Since in this case s is strictly positive, the claim follows.

Now let $\gamma(\varphi) \geq R$. Then $\Omega \cap B_R(\gamma(\varphi)\varphi)$ is contained in the cone $\mathbb{R}_{\geq 0}T_\gamma^+(\varphi)$, where

$$T_\gamma^+(\varphi) := \{\tau \in T_\gamma(\varphi) : \langle \varphi, \tau \rangle > 0\}.$$

Thus,

$$J[\gamma](\varphi) = \frac{1}{n} \int_{T_\gamma^+(\varphi)} \left[\sup\{t > 0 : t\tau \in \Omega \cap B_R(\gamma(\varphi)\varphi)\}^n - \inf\{t > 0 : t\tau \in \Omega \cap B_R(\gamma(\varphi)\varphi)\}^n \right] d\mathcal{H}^{n-1}(\tau).$$

As above we have

$$\sup\{t > 0 : t\tau \in \Omega \cap B_R(\gamma(\varphi)\varphi)\} = s(\varphi, \tau) > 0.$$

Moreover,

$$\inf\{t > 0 : t\tau \in \Omega \cap B_R(\gamma(\varphi)\varphi)\} = -s(\varphi, -\tau) > 0.$$

Since $T_\gamma(\varphi)$ is the disjoint union of $T_\gamma^+(\varphi)$ and $-T_\gamma^+(\varphi)$, the claim follows. \square

For the application of the Landweber method it is necessary to compute the adjoint $DJ[\gamma]^*$ of the derivative of J at a given function γ .

We denote by

$$\begin{aligned} T_\gamma^{(1,*)}(\varphi) &:= \{\tau \in \mathbb{S}^{n-1} : \varphi \in T_\gamma(\tau) \text{ and } \gamma(\varphi) < \langle \varphi, \tau \rangle + \eta(\tau, \varphi)\} \\ T_\gamma^{(2)}(\varphi) &:= \{\tau \in T_\gamma(\varphi) : \gamma(\tau) \geq \gamma(\varphi) \langle \varphi, \tau \rangle + \eta(\varphi, \tau)\}. \end{aligned}$$

It can be shown that

$$\begin{aligned} DJ[\gamma]^*(\beta) &= \left[\varphi \mapsto \int_{T_\gamma^{(1,*)}(\varphi)} \gamma^{n-1}(\varphi) \beta(\tau) d\mathcal{H}^{n-1}(\tau) \right. \\ &\quad \left. + \beta(\varphi) \int_{T_\gamma^{(2)}(\varphi)} |s(\varphi, \tau)|^{n-1} \left(\langle \varphi, \tau \rangle - \frac{\gamma(\varphi)(1 - \langle \varphi, \tau \rangle^2)}{\eta(\varphi, \tau)} \right) d\mathcal{H}^{n-1}(\tau) \right]. \quad (6) \end{aligned}$$

From the numerical point of view, problems arise, since the integrands are discontinuous and the second integrand may be unbounded.

Numerical experiments indicate that the functional J is not injective, if the reference point \mathbf{x}_0 is chosen to be zero, independently of γ . Therefore we consider the additional assumption $\mathbf{x}_0 = \text{cm}(\Omega)$. This assumption is incorporated in the Landweber iteration by shifting the iterate γ_i such that the center of mass of the corresponding domain Ω is zero. Note that this shift is well-defined provided the update is small enough.

Numerical Examples

The Landweber iteration was tested on the same radial functions as in the case of the cone area integral invariant. The results of the reconstruction for a relatively large circle radius $R = 2$ can be seen in Figure 2. In case of smaller radii the reconstruction works significantly worse, for too small radii the Landweber iteration does not converge. However, this may be due to discretization errors that become more pronounced with decreasing R , and also due to the regularization that has to be introduced because of the singular integrand in the adjoint (see (6)).

In the case of noisy data the circular area integral invariant provides good reconstructions with errors in the range of the noise level (see Table 2). Here, the same stopping rule has been used as for the cone invariant. The precise choice of the stopping criterion, however, turns out to be rather irrelevant. In all the cases, the norm of the residual first decreases and then immediately increases again. All stopping rules that take into account this behaviour perform similarly.

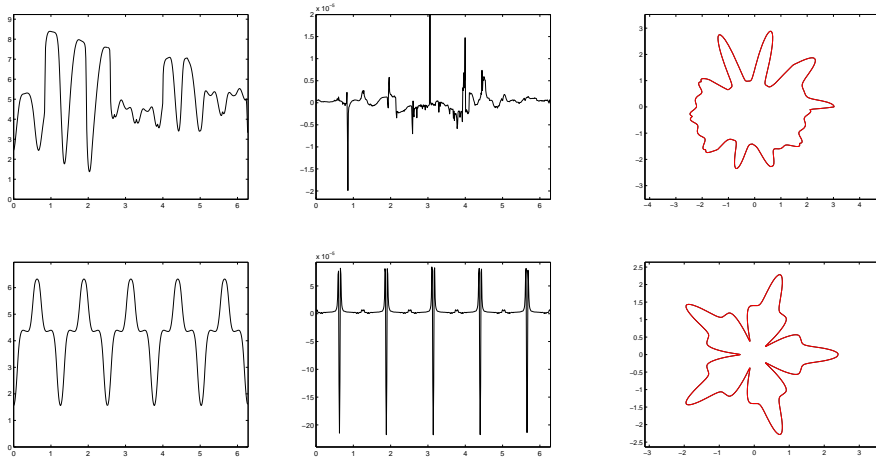


Figure 2: **(Circular area integral invariant)** *Left:* Invariant of the reconstruction. *Middle:* Residual of the invariant of the reconstruction with respect to the invariant of the original (Range: 0.1‰ of the invariant data). *Right:* Reconstructed and original curve. Parameter setting: $\mu = 0.05$, $R = 2.0$, $n_{\text{sampling points}} = 500$ and $n_{\text{iteration steps}} = 1000$.

5 Summary of the Results

The results of the Landweber iteration show that the reconstruction based upon the cone area integral invariant works well in the absence of noise (see Figure 1).

Table 2: Error measures for two different curves and several noise levels. For both curves of Figure 2 the relative L^2 - and L^∞ -error of the reconstructed radial function to the original one are listed. Parameter setting: $\mu = 0.05$ and $n_{\text{sampling points}} = 500$.

Curve	Noise Level	R	Iterations	L^2 -Error	L^∞ -Error
a	0.0%	2.0	1000	0.00013%	0.0019%
	2.5%	2.0	(121 \pm 16)	(1.90 \pm 0.08)%	(3.08 \pm 0.29)%
	5.0%	2.0	(77 \pm 16)	(3.71 \pm 0.13)%	(6.04 \pm 0.44)%
b	0.0%	2.0	1000	0.0032%	0.014%
	2.5%	2.0	(130 \pm 50)	(2.56 \pm 0.15)%	(5.37 \pm 0.95)%
	5.0%	2.0	(72 \pm 19)	(4.68 \pm 0.31)%	(8.63 \pm 1.37)%

In case of noisy data J^0 , the iteration yields reasonably good results for moderate noise levels, although the reconstruction process in general tends to produce spikes, which subsequently increases the L^∞ -error of the reconstructed radial function (see Table 1), even more in the presence of noise.

In case of the circular area integral invariant, we obtain a perfect reconstruction as long as the radius R of the defining ball is large enough. Moreover, the influence of small variations of the invariant on the reconstruction is rather small. This indicates that the invariant is well suited for describing features of a size comparable to R .

From our point of view, the quality of the numerical results give reason to focus on further investigation of integral invariants. A particularly interesting part seems to be the question of the injectivity of the circular area integral invariant, where connections to other mathematical areas can be established (see [1]).

Acknowledgement

This work has been supported by the Austrian Science Fund (FWF), Project Y123-INF, and FSP Industrial Geometry, Projects 9203-N12 and 9207-N12.

References

- [1] T. Fidler, M. Grasmair, H. Pottmann, and O. Scherzer. Inverse problems of integral invariants and shape signatures. 2007. submitted.
- [2] M. Hanke, A. Neubauer, and O. Scherzer. A convergence analysis of the Landweber iteration for nonlinear ill-posed problems. *Numer. Math.*, 72(1):21–37, 1995.
- [3] H. Krim and A. Yezzi, Jr. *Statistics and Analysis of Shapes*. Birkhäuser, Boston, 2006.
- [4] S. Manay, B. W. Hong, A. J. Yezzi, and S. Soatto. Integral invariant signatures. In [3], pages 137–166.

- [5] R. Schneider. Über eine Integralgleichung in der Theorie der konvexen Körper. *Math. Nachr.*, 44:55–75, 1970.
- [6] V.V. Volchkov. *Integral Geometry and Convolution Equations*. Kluwer Academic Publishers, Dordrecht/Boston/London, 2003.
- [7] L. Yu-Kun, Z. Qian-Yi, H. Shi-Min, J. Wallner, and H. Pottmann. Robust feature classification and editing. Submitted to IEEE TVCG, 2007.